

# Nickel(II) Complexes Bearing 4-Arylimino-1,2,3-trihydroacridines: Synthesis, Characterization, and Ethylene Oligomerization

Shengdong Wang,<sup>[a, b]</sup> Shizhen Du,<sup>[b]</sup> Wenjuan Zhang,<sup>\*[b]</sup> Sin Asuha,<sup>\*[a]</sup> and Wen-Hua Sun<sup>[b]</sup>

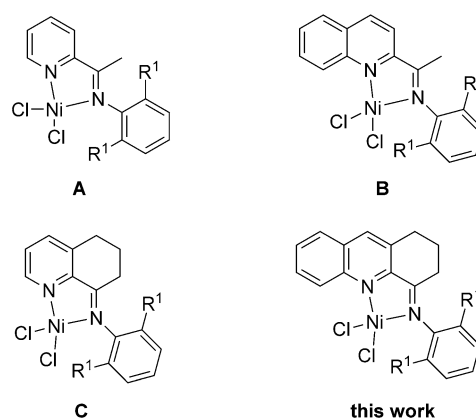
Nickel(II) complexes have attracted much attention as a new generation of olefin catalysts since the  $\alpha$ -diiminonickel complex was discovered as a highly efficient procatalyst for ethylene polymerization. A series of novel 4-arylimino-1,2,3-trihydroacridylnickel(II) dihalide complexes was synthesized in a one-pot reaction of 2,3-dihydroacridine-4-one and different anilines with nickel(II) chloride or nickel(II) bromide 1,2-dimethoxyethane complex. The complexes were characterized by infrared spectroscopy and elemental analysis. The molecular structures of the representative complexes 4-(2,6-diisopropyl-

phenylimino)-1,2,3-trihydroacridylnickel(II) dichloride (**C3**), 4-(2,4,6-trimethylphenylimino)-1,2,3-trihydroacridylnickel dichloride(II) (**C4**), and 4-(2,4,6-trimethylphenylimino)-1,2,3-trihydroacridylnickel(II) dibromide (**C9**) were confirmed by single-crystal X-ray crystallography, revealing a distorted tetrahedral geometry around the nickel(II) of **C3** and distorted trigonal bipyramidal geometry for **C4** and **C9**. With the activation of trimethylaluminum (TMA), all nickel(II) complexes exhibited good activity for ethylene oligomerization, and oligomer products ranged from butene ( $C_4$ ) to hexadecene ( $C_{16}$ ).

## Introduction

Since the discovery of the  $\alpha$ -diiminonickel(II) complex as a highly efficient procatalyst for ethylene polymerization,<sup>[1]</sup> the design of nickel(II) complexes has attracted much attention in the past decades. Many groups joined this research area and designed numerous new *N,N*-bidentate nickel(II) complexes for ethylene polymerization.<sup>[2]</sup> The majority of ligands reported in literature are  $\alpha$ -diimine derivatives, and the examples of iminopyridylnickel(II) complexes are still rare.

Our group focused on the design and synthesis of new late transition metal complexes for ethylene polymerization, and recently, we reviewed the progress of the use of nickel(II) and iron complexes in ethylene polymerization.<sup>[3]</sup> Many results indicated that catalytic properties greatly depended on the backbone and substituents of the ligands, which provided different coordination environments for metals. For example, 2-iminopyridylnickel(II) complexes **A** (Scheme 1) ( $R^1 = \text{Me, Et, } i\text{Pr}$ ) cata-



Scheme 1. *N,N*-bidentate nickel(II) complexes.

lyzed ethylene polymerization and produced oligomers and polymers.<sup>[4]</sup> With increased steric hindrance of the substituent, such as having a dibenzhydryl group on the *ortho* position of the phenyl group or a dibenzhydrylnaphthyl group on the imino nitrogen atom, the resultant nickel(II) complexes showed a much higher activity (up to  $10^7 \text{ g mol}^{-1} (\text{Ni}) \text{ h}^{-1}$ ). They also produced only polyethylene (PE) wax with a narrow molecular weight distribution, with the molecular weight ranging from several hundreds to thousands.<sup>[5,6]</sup>

With a benzene ring fused to the pyridine ring, the resultant nickel(II) complexes **B** bearing 2-(1-aryliminoethylidene)quinolines exhibited a good activity for ethylene oligomerization ( $10^6 \text{ g mol}^{-1} (\text{Ni}) \text{ h}^{-1}$ ) at a higher optimal temperature of  $80^\circ \text{C}$ . This indicates better thermal stability, and the oligomer product ranged from  $C_4$  (butene) to  $C_{20}$ .<sup>[7a]</sup> Adding a further sub-

[a] S. Wang, Prof. Dr. S. Asuha

Chemistry & Environment Science College, Inner Mongolia Normal University, and Key Laboratory of Physics & Chemistry of Functional Materials Inner Mongolia, 81 Zhaowudalu, Huhhot 010022 (P. R. China)  
E-mail: asuha@imnu.edu.cn

[b] S. Wang, S. Du, Prof. Dr. W. Zhang, Prof. Dr. W.-H. Sun

Key Laboratory of Engineering Plastics and Beijing National Laboratory for Molecular Sciences Institute of Chemistry, Chinese Academy of Science Beijing 100190 (P. R. China)  
E-mail: zhangwj@iccas.ac.cn

Supporting information for this article is available on the WWW under <http://dx.doi.org/10.1002/open.201402113>.

© 2014 The Authors. Published by Wiley-VCH Verlag GmbH & Co. KGaA. This is an open access article under the terms of the Creative Commons Attribution-NonCommercial-NoDerivs License, which permits use and distribution in any medium, provided the original work is properly cited, the use is non-commercial and no modifications or adaptations are made.

stituent (Me, Et, *i*Pr) to the 8-position of quinoline, we obtained nickel(II) complexes that can only catalyze the ethylene dimerization at 20 °C, even in the case of a very bulky dibenzhydryl group at the 2,6-position of phenyl ring.<sup>[7b]</sup> The above examples demonstrate the structure of the backbone has more influence than the substituents within the phenyl ring when it comes to the catalytic behavior of the complexes towards ethylene polymerization, and the incorporation of a benzene ring to pyridine switches the ethylene polymerization to oligomerization. The reason for such a phenomenon is probably the increased electron density at the nickel(II) center due to conjugation, which leads to the decreased activity and the product of much lower molecular weight.

On the contrary, the nickel(II) complexes containing fused-cycloalkanonylpyridines, such as 8-arylimino-5,6,7-trihydroquinoline complexes **C**, showed high activities for ethylene polymerization (up to  $10^7 \text{ g mol}^{-1} (\text{Ni}) \text{ h}^{-1}$ ) without any oligomers.<sup>[8a,b]</sup> Even after incorporating a strong electron-withdrawing group such as  $\text{NO}_2$  into the phenyl ring, the polymerization by **C** still reaches  $4.0 \times 10^6 \text{ g mol}^{-1} (\text{Ni}) \text{ h}^{-1}$  without any oligomers produced.<sup>[8c]</sup> These results suggest that the cycloketonyl group fused to pyridine led to increased ethylene polymerization activity, compared with the results using iminopyridylnickel(II) complexes **A**.

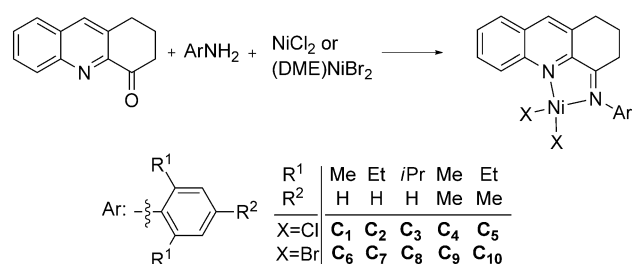
In order to further investigate the effects of the benzene ring and cycloketonyl group fused to pyridine on the catalytic activity of the complex, we designed and prepared 4-arylimino-1,2,3-trihydroacridylnickel(II) dihalides and investigated their catalytic behavior towards ethylene reactivity in detail.

## Results and Discussion

### Synthesis and characterization of 4-arylimino-1,2,3-trihydroacridylnickel(II) dihalides

Firstly, the individual mixtures of the 2,3-dihydroacridine-4-one with anilines in toluene were refluxed for several hours to prepare the corresponding Schiff bases. The products could be observed by thin layer chromatography (TLC); however, the isolation and purification of these compounds always failed due to their easy decomposition. Therefore, the target nickel(II) complexes were synthesized using the one-pot process, in which the mixtures of 2,3-dihydroacridin-4-one and the corresponding anilines together with nickel(II) chloride or nickel(II) bromide–1,2-dimethoxyethane (DME) complex were refluxed in acetic acid (Scheme 2). The complexes were then isolated and characterized by Fourier transform infrared (FTIR) spectroscopy and elemental analysis. Their FTIR spectra showed a strong band in the range of  $1600\text{--}1630 \text{ cm}^{-1}$  which can be ascribed to the stretching vibration of  $\text{C}=\text{N}$ . All the nickel(II) complexes are stable in both solution and solid state.

Single crystals of **C3**, **C4**, and **C9** suitable for X-ray analysis were obtained by layering diethyl ether on their methanol solutions at room temperature. The molecular structures are shown in Figure 1 a–c, and selected bond lengths and angles are listed in Table 1.



**Scheme 2.** Synthetic procedure for 4-arylimino-1,2,3-trihydroacridylnickel(II) dihalides. (See Experimental Section for specific reagents, conditions, and yields for the ten complexes.)

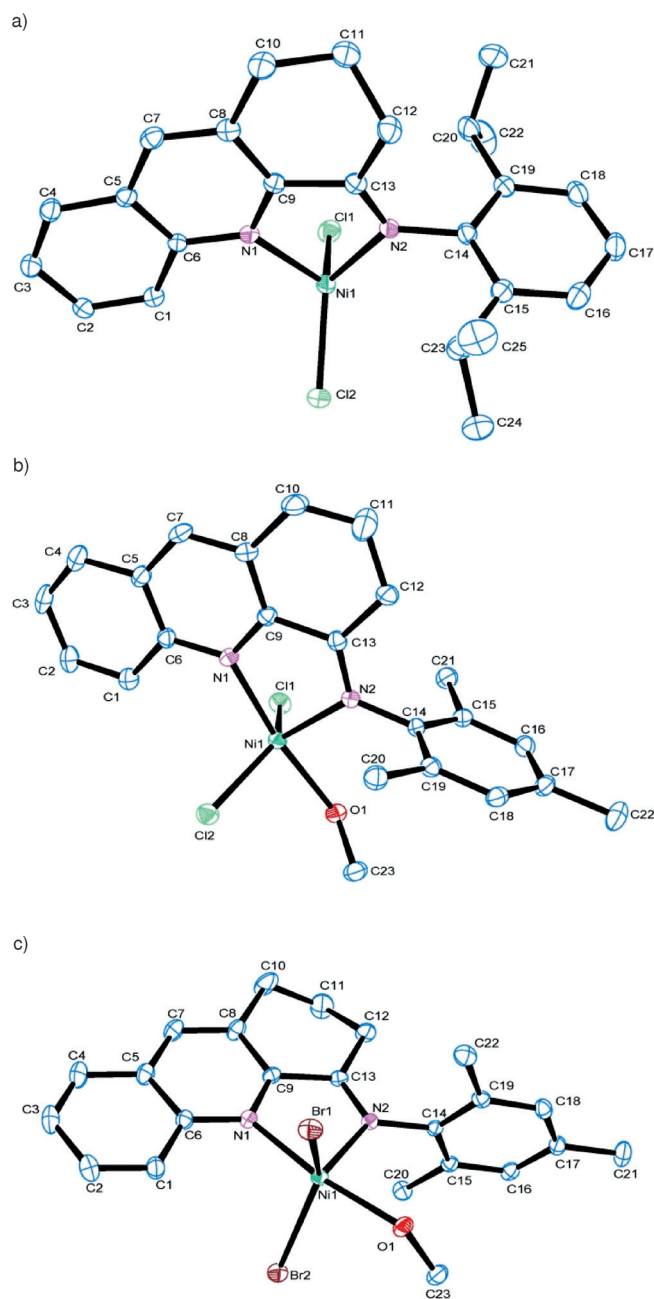


**Figure 1.** Molecular structure of a) **C3**, b) **C4-CH<sub>3</sub>OH**, and c) **C9-CH<sub>3</sub>OH**. Thermal ellipsoids are shown at 30% probability. Hydrogen atoms have been omitted for clarity.

**Table 1.** Selected bond lengths and angles for **C3**, **C4-CH<sub>3</sub>OH**, and **C9-CH<sub>3</sub>OH**.

	<b>C3</b> (X = Cl)	<b>C4-CH<sub>3</sub>OH</b> (X = Cl)	<b>C9-CH<sub>3</sub>OH</b> (X = Br)
Bond lengths [Å]			
Ni1–N1	1.9979(19)	2.082(3)	2.082(3)
Ni1–N2	2.0014(19)	2.037(3)	2.022(2)
Ni1–X1	2.2210(9)	2.2819(12)	2.4332(8)
Ni1–X2	2.1885(8)	2.3046(14)	2.4432(7)
N1–C6	1.363(3)	1.369(4)	1.363(4)
N1–C9	1.332(3)	1.328(4)	1.327(4)
N2–C13	1.283(3)	1.280(4)	1.285(4)
N2–C14	1.448(3)	1.444(4)	1.453(4)
Bond angles [°]			
N2–Ni1–N1	81.92(8)	79.63(12)	79.75(11)
N1–Ni1–X1	105.03(6)	92.76(9)	92.76(8)
N1–Ni1–X2	112.01(6)	94.24(9)	94.53(7)
N2–Ni1–X1	106.20(6)	111.17(9)	111.95(7)
N2–Ni1–X2	119.79(6)	116.47(9)	115.67(7)
X1–Ni1–X2	123.42(4)	132.34(5)	132.36(3)
N1–Ni1–O1		172.23(10)	172.03(10)

Figure 1a shows **C3** has tetrahedral geometry around the nickel(II) center, and two nitrogen and two chlorine atoms are coordinated to nickel(II), which is a very common coordination model for nickel(II) complexes. The bond lengths of Ni–Cl are 2.2210(9) Å and 2.1885(8) Å, which are quite similar to other nickel(II) complexes.<sup>[4,7]</sup> The N1–C9–C13–N2 coordination plane and C1–C2–C3–C4 quinoline plane are almost coplanar, and their dihedral angle is 8.18°, while the dihedral angle between the C10–C11–C12 plane and coordination plane is about 51.33°.

Figure 1b shows **C4** has a different coordination model than **C3**, in which one methanol molecule is coordinated to nickel(II), and the complex possesses distorted trigonal bipyramidal geometry. Two chlorides occupy the axial positions, and the distances between them and the N2–N1–Ni1–O1 coordination plane are 2.126 Å and 2.067 Å. In addition, the dihedral angle between the coordination plane and the quinoline is 6.88°, and another dihedral angle between the C12–C11–C10 plane and the N2–N1–Ni1–O1 coordination plane is equal to 38.13°. Due to weaker electron donation of the methyl group as compared with the isopropyl group, the bond lengths of Ni–Cl1, Ni1–Cl2, Ni1–N1, and Ni1–N2 in **C4** (2.2819(12) Å, 2.3046(14) Å, 2.082(3) Å, 2.037(3) Å, respectively) are much longer than those in **C3** (2.2210(9) Å, 2.1885(8) Å, 1.9979(19) Å, 2.0014(19) Å, respectively). This may provide the possibility of coordination of the solvent to the nickel(II) center. The above results indicate the substituent on the *ortho* position of the aryl probably affects the coordination model.

Figure 1c shows **C9** has quite a similar structure to that of **C4**. One methanol is coordinated to the nickel(II) center, and the complex possesses distorted trigonal bipyramidal geometry around nickel(II). The benzene ring was almost perpendicular to the Ni–N1–N2 coordination plane, with a dihedral angle of 84.5°. The dihedral angle between the C12–C11–C10 plane and N2–N1–Ni1 plane is 38.12°. The distances of the two

chlorides to the N2–N1–Ni1–O1 coordination plane are 2.256 Å and 2.202 Å. The bond lengths of Ni–N (2.082(3) Å and 2.022(2) Å) are quite close to those of **C4**, while the Ni–Br bond lengths are much longer than those for Ni–Cl, probably due to the larger radius of Br. This affects their catalytic activities, which are demonstrated in the polymerization investigation.

## Ethylene oligomerization

### Ethylene oligomerization by nickel(II) complexes **C1–C5**

The catalytic properties of the complexes for ethylene polymerization were investigated in detail, and the polymerization results are summarized in Table 2. With the activation of different cocatalysts such as methylaluminoxane (MAO), modified methylaluminoxane (MMAO), dimethylaluminum chloride, and

**Table 2.** Ethylene oligomerization by nickel(II) chloride complexes **C1–C5**.<sup>[a]</sup>

Run	Complex	Cocatalyst	Al/Ni	Temp [°C]	Activity <sup>[b]</sup>	Oligomer distribution <sup>[c]</sup> [%]		
						C <sub>4</sub> /ΣC	C <sub>6</sub> /ΣC	≥ C <sub>6</sub> /ΣC
1	<b>C3</b>	MMAO	1000	30	3.67	37.9	22.4	39.7
2	<b>C3</b>	MAO	1000	30	2.41	22.3	8.1	69.6
3	<b>C3</b>	Me <sub>2</sub> AlCl	300	30	4.21	20.6	10.5	68.9
4	<b>C3</b>	TMA	300	30	4.95	41.1	15.3	43.6
5	<b>C3</b>	TMA	300	20	3.86	36.5	13.6	49.9
6	<b>C3</b>	TMA	300	40	3.79	43.0	9.6	47.4
7	<b>C3</b>	TMA	300	50	1.71	47.9	5.1	47.0
8	<b>C3</b>	TMA	200	30	2.11	35.9	10.4	54.7
9	<b>C3</b>	TMA	250	30	3.44	38.2	6.5	55.3
10	<b>C3</b>	TMA	350	30	3.84	42.0	12.9	45.1
11	<b>C3</b>	TMA	400	30	3.55	43.8	15.3	40.9
12 <sup>[d]</sup>	<b>C3</b>	TMA	300	30	6.33	42.1	12.8	45.1
13 <sup>[e]</sup>	<b>C3</b>	TMA	300	30	4.39	31.7	6.7	61.6
14 <sup>[f]</sup>	<b>C3</b>	TMA	300	30	2.63	31.5	9.3	59.2
15	<b>C1</b>	TMA	300	30	6.50	43.9	13.5	42.6
16	<b>C2</b>	TMA	300	30	5.31	46.4	6.6	47.0
17	<b>C4</b>	TMA	300	30	8.36	37.7	10.1	52.2
18	<b>C5</b>	TMA	300	30	5.74	48.7	9.3	42.0

[a] Reagents and conditions: Ni (4 μmol), ethylene (10 atm), toluene (100 mL), 30 min; [b] unit: 10<sup>5</sup> g mol<sup>-1</sup> (Ni) h<sup>-1</sup>; [c] Determined by GC. ΣC denotes the total amount of oligomers; [d] 15 min; [e] 45 min; [f] 60 min.

trimethylaluminum (TMA), nickel(II) complex **C3** showed moderate activity for ethylene oligomerization, and products ranged from C<sub>4</sub> to C<sub>16</sub>, with butene as the major product. The best activities were achieved with TMA as cocatalyst, which was selected for further tests described below.

As 2-aryliminoquinolynickel(II) complexes showed good activity for ethylene oligomerization at 80°C under the activation of diethylaluminum chloride,<sup>[7a]</sup> we investigated the temperature effect on reactivity. Results show the highest activity was achieved at 30°C for the **C3**/TMA catalytic system (runs 4–7, Table 2). When we elevated the temperature from 20°C to 50°C, the C<sub>4</sub>/ΣC increased from 36.5% to 47.9%, which, as

usual, suggested the higher relative rate of chain transfer with respect to chain propagation at a higher temperature.

At the optimized temperature of 30 °C, the effects of the Al/Ni ratio and the reaction time were also investigated. The highest activity was achieved at a molar ratio of 300, though the activity had no big difference with different amounts of TMA. The  $C_4/\Sigma C$  value increased slightly from 35.9 to 43.8% when the amount of cocatalyst is increased (runs 4, 8–11, Table 2), suggesting a lower rate of chain propagation compared with chain transfer at a higher TMA concentration.<sup>[1b,9]</sup> Prolonging the reaction time leads to the decrease of the reactivity as usual, which could be explained by the deactivation of active species. Meanwhile, the  $C_4/\Sigma C$  value decreased, and the amount of other longer oligomer products increased, which can be explained by faster chain propagation than chain transfer at longer reaction times.

The effect of ligand environment on the catalytic properties of the complexes was also investigated under the optimized conditions. Generally, smaller substituents lead to higher activity, which is demonstrated by the reactivity order: **C1** ( $R^1 = \text{Me}$ ) > **C2** ( $R^1 = \text{Et}$ ) > **C3** ( $R^1 = i\text{Pr}$ ). The results indicate that bulkier substituents on the *ortho*-position of the benzene ring preclude the ethylene insertion and lead to lower activity. These results are quite similar to previous ones involving 2-(1-aryl-iminoethylidene)quinoline nickel(II) complexes **B** (Scheme 1).<sup>[7a]</sup>

Nickel(II) complexes **C** bearing 8-arylimino-5,6,7-trihydroquinolines (Scheme 1) exhibited quite high activities in ethylene polymerization and produced polyethylene wax with narrow distribution,<sup>[8]</sup> but in this case the incorporation of the benzene ring leads to a much lower activity in ethylene oligomerization.

### Ethylene oligomerization by nickel(II) complexes **C6–C10**

The catalytic properties of nickel(II) complexes **C6–C10** were also investigated, and the results are collected in Table 3. Firstly, by using **C8**, the optimal cocatalyst was identified; the **C8**/TMA system shows the highest activity for ethylene oligomerization (runs 1–4, Table 3). Then the effects of the Al/Ni ratio, temperature, and reaction time were studied by using the **C8**/TMA catalyst system. The optimum conditions are 30 °C with an Al/Ni molar ratio of 300, which is the same as for **C3**/TMA.

Contrary to the results for **C3**/TMA, for the **C8**/TMA system, the trend of  $C_4/\Sigma C$  agrees with the trend of the activity seen when the temperature and Al/Ni molar ratio are increased. For example, when increasing the Al/Ni molar ratio from 200 to 300, the activity increases from  $3.08 \times 10^5$  to  $6.31 \times 10^5 \text{ g mol}^{-1} (\text{Ni}) \text{ h}^{-1}$ , while the  $C_4/\Sigma C$  also slightly increases from 40.3 to 47.5%. Further increasing the molar ratio from 300 to 400 leads to the decrease in activity from  $6.31 \times 10^5$  to  $4.04 \times 10^5 \text{ g mol}^{-1} (\text{Ni}) \text{ h}^{-1}$  and the decrease of  $C_4/\Sigma C$  from 47.5 to 32.2%, suggesting different active species and metal coordination environments compared with those for the **C3**/TMA catalyst system.

Prolonging the reaction time leads to lower activity (runs 4, 12–14, Table 3), which is in good agreement with the majority of literature reports,<sup>[10]</sup> and indicates the deactivation of active

**Table 3.** Ethylene oligomerization by nickel(II) bromide complexes **C6–C10**.<sup>[a]</sup>

Run	Complex	Cocatalyst	Al/Ni	Temp [°C]	Activity <sup>[b]</sup>	Oligomer distribution <sup>[c]</sup> [%]		
						$C_4/\Sigma C$	$C_6/\Sigma C$	$\geq C_6/\Sigma C$
1	<b>C8</b>	MMAO	1000	30	5.53	30.5	20.3	49.2
2	<b>C8</b>	MAO	1000	30	3.32	38.4	12.5	49.1
3	<b>C8</b>	Me <sub>2</sub> AlCl	300	30	5.80	20.1	13.3	66.6
4	<b>C8</b>	TMA	300	30	6.31	47.5	17.6	34.9
5	<b>C8</b>	TMA	300	20	4.38	33.2	9.7	57.1
6	<b>C8</b>	TMA	300	40	5.13	39.5	10.3	50.2
7	<b>C8</b>	TMA	300	50	2.27	38.7	7.6	53.7
8	<b>C8</b>	TMA	200	30	3.08	40.3	6.6	53.1
9	<b>C8</b>	TMA	250	30	4.89	44.9	8.6	46.5
10	<b>C8</b>	TMA	350	30	5.05	34.6	12.1	53.3
11	<b>C8</b>	TMA	400	30	4.04	32.2	13.3	54.5
12 <sup>[d]</sup>	<b>C8</b>	TMA	300	30	9.31	36.7	9.7	53.6
13 <sup>[e]</sup>	<b>C8</b>	TMA	300	30	5.83	35.3	11.2	53.5
14 <sup>[f]</sup>	<b>C8</b>	TMA	300	30	2.32	31.2	12.8	56.0
15	<b>C6</b>	TMA	300	30	7.31	43.3	8.9	47.8
16	<b>C7</b>	TMA	300	30	6.83	39.7	12.3	48.0
17	<b>C9</b>	TMA	300	30	9.35	37.3	10.2	52.5
18	<b>C10</b>	TMA	300	30	7.22	40.2	6.3	53.5

[a] Reagents and conditions: Ni (4 μmol), ethylene (10 atm), toluene (100 mL), 30 min; [b] unit:  $10^5 \text{ g mol}^{-1} (\text{Ni}) \text{ h}^{-1}$ ; [c] Determined by GC.  $\Sigma C$  denotes the total amount of oligomers; [d] 15 min; [e] 45 min; [f] 60 min.

species. In addition, the proportion of longer oligomer products increases.

Under the same conditions, nickel(II) bromide complexes **C6–C10** (runs 4, 15–18 in Table 3) generally show higher activities [ $6.31\text{--}9.75 \times 10^5 \text{ g mol}^{-1} (\text{Ni}) \text{ h}^{-1}$ ] than the corresponding nickel(II) chloride analogues **C1–C5** [ $4.95\text{--}8.36 \times 10^5 \text{ g mol}^{-1} (\text{Ni}) \text{ h}^{-1}$ ] (runs 4, 15–18, in Table 2). The reason is probably the much longer distance of Ni–Br than Ni–Cl, which facilitates halogen atom abstraction by trimethylaluminum. Compared with **C1–C5**, the **C6–C10** complexes show quite similar effects of ligand environment on activity, which is demonstrated by the same activity order: **C6** ( $R^1 = \text{Me}$ ) > **C7** ( $R^1 = \text{Et}$ ) > **C8** ( $R^1 = i\text{Pr}$ ). In addition, the incorporation of *p*-methyl within the benzene ring increases the activity, as demonstrated by the activity order: **C9** ( $R^1 = R^2 = \text{Me}$ ) > **C6** ( $R^1 = \text{Me}$ ) and **C10** ( $R^1 = \text{Me}, R^2 = \text{Et}$ ) > **C7** ( $R^1 = \text{Et}$ ), which is the same as the case of **C1–C5**.

## Conclusions

A series of novel 4-arylimino-1,2,3-trihydroacridylnickel(II) dihalides was prepared by one-pot synthesis and characterized by elemental analysis and FTIR spectroscopy. With the activation of trimethylaluminum (TMA), all nickel(II) complexes exhibit good activity for ethylene oligomerization with the oligomer products ranging from  $C_4$  to  $C_{16}$ . Comparing current results with those obtained by 2-aryliminoquinolynickel(II) complexes **B**, we can state that the replacement of the acetyl group with a cycloketonyl group has no big effect on reactivity and the product. In contrast, further comparisons with the results obtained by 8-arylimino-5,6,7-trihydroquinoline nickel(II) halides **C** (Scheme 1) lead to the observation that the introduction

of a phenyl group into quinoline in this work switches ethylene polymerization to oligomerization with lower activity. This further demonstrates the assumption that a larger conjugated structure in the backbone decreases the activity of the complex and the molecular weight of the product. The above results provide important information for understanding the relationship between the backbone of ligands and ethylene reactivity. This study is also a step towards designing highly efficient nickel(II) complexes for ethylene polymerization in the future.

## Experimental Section

### General considerations

Manipulation of air and/or moisture-sensitive compounds was done under a high-purity N<sub>2</sub> atmosphere using standard Schlenk techniques. Toluene was routinely purified and distilled over Na before use. 1,2-dimethoxyethane (DME)–NiBr<sub>2</sub> complex was synthesized by the reaction of DME with anhydrous NiBr<sub>2</sub>. Methylaluminoxane (MAO, 1.46 M solution in toluene) and modified methylaluminoxane (MMAO, 1.93 M in *n*-heptane) were purchased from AkzoNobel. Trimethylaluminum (TMA, 1.00 M in toluene) was purchased from Aldrich. Me<sub>2</sub>AlCl (1.00 M in toluene) and other reagents were purchased from Acros Chemicals or local suppliers. Elemental analysis was completed by using a Flash EA 1112 micro-analyzer (Thermo Fisher Scientific, Waltham, USA). FTIR spectra were determined by a System 2000 FTIR spectrometer (PerkinElmer, Waltham, USA). Gas chromatography (GC) analysis was performed with a CP-3800 gas chromatograph (Varian, Palo Alto, USA) equipped with a flame ionization detector and a 30 m column (0.2 mm internal diameter, 0.25 μm film thickness).

### Synthesis and characterization of complexes C1–C10

**4-(2,6-dimethylphenylimino)-1,2,3-trihydroacridylnickel(II) dichloride (C1):** The raw materials 2,3-dihydroacridin-4(1*H*)-one (1.0 mmol) and NiCl<sub>2</sub>·6H<sub>2</sub>O (1.0 mmol) were dissolved in glacial HOAc (10 mL), and 2,6-dimethylbenzenamine (1.0 mmol) was added into the solution. The mixture was held at reflux for 3 h. The solvent was removed under vacuum, and CH<sub>3</sub>OH (10 mL) was added to dissolve the residue. Unreacted NiCl<sub>2</sub> was removed by filtration. Then diethyl ether (50 mL) was added to afford a yellow precipitate from the solution. After filtration and washing with diethyl ether (3 × 5 mL), the yellow powder was collected and dried under vacuum at rt. **C1** was obtained as a yellow powder (344.4 mg, 80.1%); FTIR (KBr):  $\tilde{\nu}$  = 3061, 2910, 2879, 2850, 1622, 1565, 1498, 1448, 1382, 1349, 1312, 1213, 1171, 989, 961, 923, 843, 781, 754, 677 cm<sup>-1</sup>; Anal. calcd for C<sub>21</sub>H<sub>20</sub>C<sub>12</sub>N<sub>2</sub>Ni (430.00): C 58.66, H 4.69, N 6.51, found: C 58.48, H 4.63, N 6.40.

**4-(2,6-diethylphenylimino)-1,2,3-trihydroacridylnickel(II) dichloride (C2):** In the same manner as the synthesis of **C1**, **C2** was obtained as a yellow powder (366.9 mg, 80.1%); FTIR (KBr):  $\tilde{\nu}$  = 2959, 2926, 2863, 1617, 1564, 1498, 1447, 1348, 1311, 1211, 1170, 1026, 961, 922, 786, 755, 709, 678 cm<sup>-1</sup>; Anal. calcd for C<sub>23</sub>H<sub>24</sub>C<sub>12</sub>N<sub>2</sub>Ni (458.05): C 60.31, H 5.28, N 6.12, found: C 59.81, H 5.21, N 5.94.

**4-(2,6-diisopropylphenylimino)-1,2,3-trihydroacridylnickel(II) dichloride (C3):** In the same manner as the synthesis of **C1**, **C3** was obtained as a red powder (361.7 mg, 74.4%); FTIR (KBr):  $\tilde{\nu}$  = 3075, 2962, 2928, 2863, 1618, 1564, 1496, 1447, 1384, 1355, 1315, 1214, 1171, 1147, 1103, 973, 930, 845, 807, 783, 757 cm<sup>-1</sup>; Anal. calcd for

C<sub>25</sub>H<sub>28</sub>Cl<sub>2</sub>N<sub>2</sub>Ni (486.10): C 61.77, H 5.81, N 5.76, found: C 61.34, H 5.78, N 5.59.

**4-(2,4,6-trimethylphenylimino)-1,2,3-trihydroacridylnickel(II) dichloride (C4):** In the same manner as the synthesis of **C1**, **C4** was obtained as a yellow powder (377.8 mg, 85.1%); FTIR (KBr):  $\tilde{\nu}$  = 3362, 3050, 2943, 2856, 1615, 1564, 1496, 1458, 1385, 1349, 1309, 1216, 1178, 1150, 1006, 925, 852, 791, 748, 680 cm<sup>-1</sup>; Anal. calcd for C<sub>22</sub>H<sub>22</sub>Cl<sub>2</sub>N<sub>2</sub>Ni (444.02): C 59.51, H 4.99, N 6.31, found: C 59.72, H 5.01, N 6.21.

**4-(2,6-diethyl-4-methylphenylimino)-1,2,3-trihydroacridylnickel(II) dichloride (C5):** In the same manner as the synthesis of **C1**, **C5** was obtained as a yellow powder (344.1 mg, 72.9%); FTIR (KBr):  $\tilde{\nu}$  = 3048, 2925, 2865, 1628, 1565, 1494, 1455, 1350, 1313, 1214, 1147, 1018, 958, 927, 856, 786, 746 cm<sup>-1</sup>; Anal. calcd for C<sub>24</sub>H<sub>26</sub>Cl<sub>2</sub>N<sub>2</sub>Ni (472.08): C 61.06, H 5.55, N 5.93, found: C 60.83, H 5.44, N 6.05.

**4-(2,6-dimethylphenylimino)-1,2,3-trihydroacridylnickel(II) dibromide (C6):** The raw materials 2,3-dihydroacridin-4(1*H*)-one (1.0 mmol), and (DME)NiBr<sub>2</sub> (1.0 mmol) were dissolved in glacial HOAc (10 mL), and 2,6-dimethylbenzenamine (1.0 mmol) was added into the solution. The mixture was held at reflux for 3 h. The solvent was removed under vacuum, and CH<sub>3</sub>OH (10 mL) was added to dissolve the residue. Unreacted (DME)NiBr<sub>2</sub> was removed by filtration. Then diethyl ether (50 mL) was added to get the precipitate which was collected by filtration and washed with diethyl ether (3 × 5 mL). After drying under vacuum at rt, **C6** was obtained as a yellow powder (381.4 mg, 73.5%); FTIR (KBr):  $\tilde{\nu}$  = 2946, 2908, 2860, 1629, 1586, 1497, 1439, 1383, 1348, 1307, 1212, 927, 781, 758, 677 cm<sup>-1</sup>; Anal. calcd for C<sub>21</sub>H<sub>20</sub>Br<sub>2</sub>N<sub>2</sub>Ni (518.90): C 48.61, H 3.88, N 5.40, found: C 48.94, H 3.92, N 5.35.

**4-(2,6-diethylphenylimino)-1,2,3-trihydroacridylnickel(II) dibromide (C7):** In the same manner as the synthesis of **C6**, **C7** was obtained as a yellow powder (408.6 mg, 74.7%); FTIR (KBr):  $\tilde{\nu}$  = 2962, 2923, 2875, 1615, 1562, 1494, 1446, 1347, 1310, 1210, 1054, 921, 781, 752, 708 cm<sup>-1</sup>; Anal. calcd for C<sub>23</sub>H<sub>24</sub>Br<sub>2</sub>N<sub>2</sub>Ni (546.95): C 50.51, H 4.42, N 5.12, found: C 50.05, H 4.12, N 4.89.

**4-(2,6-diisopropylphenylimino)-1,2,3-trihydroacridylnickel(II) dibromide (C8):** In the same manner as the synthesis of **C6**, **C8** was obtained as a yellow powder (400.8 mg, 69.7%); FTIR (KBr):  $\tilde{\nu}$  = 2962, 2926, 2866, 1616, 1562, 1496, 1447, 1384, 1354, 1313, 1216, 1170, 1148, 1102, 1052, 928, 782, 756 cm<sup>-1</sup>; Anal. calcd for C<sub>25</sub>H<sub>28</sub>Br<sub>2</sub>N<sub>2</sub>Ni (575.00): C 52.22, H 4.91, N 4.87, found: C 52.25, H 4.79, N 4.93.

**4-(2,4,6-trimethylphenylimino)-1,2,3-trihydroacridylnickel(II) dibromide (C9):** In the same manner as the synthesis of **C6**, **C9** was obtained as a yellow powder (344.3 mg, 64.6%); FTIR (KBr):  $\tilde{\nu}$  = 3361, 2938, 2867, 1612, 1564, 1498, 1456, 1347, 1308, 1217, 1151, 1090, 1002, 923, 857, 789, 756, 679 cm<sup>-1</sup>; Anal. calcd for C<sub>22</sub>H<sub>22</sub>Br<sub>2</sub>N<sub>2</sub>Ni (532.92): C 49.58, H 4.16, N 5.26, found: C 49.52, H 4.58, N 5.01.

**4-(2,6-diethyl-4-methylphenylimino)-1,2,3-trihydroacridylnickel(II) dibromide (C10):** In the same manner as the synthesis of **C6**, **C10** was obtained as a yellow powder (366.3 mg, 65.3%); FTIR (KBr):  $\tilde{\nu}$  = 2963, 2871, 1618, 1562, 1498, 1454, 1382, 1350, 1308, 1213, 1177, 1150, 1025, 925, 870, 786, 748, 683 cm<sup>-1</sup>; Anal. calcd for C<sub>24</sub>H<sub>26</sub>Br<sub>2</sub>N<sub>2</sub>Ni (560.98): C 51.38, H 4.67, N 4.99, found: C 51.35, H 4.59, N 4.90.

### General procedure for ethylene oligomerization at 10 atm of ethylene pressure

Ethylene oligomerization at constant ethylene pressure was performed in a 0.25 L stainless steel autoclave equipped with a mechanical stirrer and a temperature controller. The reactor was heated in vacuum at 80 °C and recharged with ethylene three times before the reaction. The nickel(II) precatalyst was dissolved in toluene (50 mL) using standard Schlenk techniques and injected into the reactor under an ethylene atmosphere. When the oligomerization temperature was reached, the required amount of cocatalyst and the residual toluene (the total toluene was 100 mL) was injected into the reactor. A pressure of 10 atm ethylene was immediately reached to start the reaction, and the ethylene feed was kept for constant pressure throughout the reaction time. When the reaction was completed, 1 mL of the reaction solution was quenched by the addition of 10% aqueous HCl. The organic layer was collected for GC analysis to determine the distribution of oligomers obtained.

**Table 4.** Crystallographic data and refinement details for complexes **C3**, **C4-CH<sub>3</sub>OH**, and **C9-CH<sub>3</sub>OH**.

	<b>C3</b>	<b>C4-CH<sub>3</sub>OH</b>	<b>C9-CH<sub>3</sub>OH</b>
Empirical formula	C <sub>25</sub> H <sub>28</sub> Cl <sub>2</sub> N <sub>2</sub> Ni	C <sub>23</sub> H <sub>25</sub> Cl <sub>2</sub> N <sub>2</sub> NiO	C <sub>23</sub> H <sub>25</sub> Br <sub>2</sub> N <sub>2</sub> NiO
Formula weight	486.10	475.06	563.98
Crystal color	red	yellow	yellow
Temp [K]	173(2)	173(2)	173(2)
Wavelength [Å]	0.71073	0.71073	0.71073
Crystal system	Monoclinic	Triclinic	Triclinic
Space group	P2(1)/n	P-1	P-1
a [Å]	10.025(2)	9.838(2)	9.946(2)
b [Å]	17.024(3)	11.685(2)	11.947(2)
c [Å]	13.434(3)	11.772(2)	11.993(2)
α [°]	90	117.50(3)	114.41(3)
β [°]	90.48(3)	106.93(3)	112.80(3)
γ [°]	90	97.98(3)	96.93(3)
Volume [Å <sup>3</sup> ]	2292.6(8)	1087.2(3)	1127.4(3)
Z	4	2	2
Density calcd [mg m <sup>-3</sup> ]	1.408	1.451	1.661
μ [mm <sup>-1</sup> ]	1.094	1.155	4.421
F(000)	1016	494	566
Crystal size [mm]	0.79 × 0.23 × 0.18	0.26 × 0.11 × 0.04	0.63 × 0.16 × 0.12
θ range [°]	2.36–27.51	3.21–27.49	2.29–27.50
Limiting indices	–12 ≤ h ≤ 13 –22 ≤ k ≤ 22 –17 ≤ l ≤ 17	–12 ≤ h ≤ 12 –15 ≤ k ≤ 14 –15 ≤ l ≤ 15	–12 ≤ h ≤ 12 –15 ≤ k ≤ 15 –15 ≤ l ≤ 15
No. of rflns collected	16 359	13 856	14 514
No. unique rflns	5230	4961	5140
R(int)	0.0510	0.0604	0.0594
Completeness to θ [%]	99.4	99.4	99.4
Goodness of fit on F <sup>2</sup>	1.157	1.046	1.096
Final R indices [I > 2σ(I)]	R <sub>1</sub> = 0.0485 wR <sub>2</sub> = 0.1113	R <sub>1</sub> = 0.0592 wR <sub>2</sub> = 0.1633	R <sub>1</sub> = 0.0412 wR <sub>2</sub> = 0.1033
R indices (all data)	R <sub>1</sub> = 0.0517 wR <sub>2</sub> = 0.1135	R <sub>1</sub> = 0.0699 wR <sub>2</sub> = 0.1749	R <sub>1</sub> = 0.0446 wR <sub>2</sub> = 0.1056
Largest diff peak and hole [e Å <sup>-3</sup> ]	0.447 and –0.414	1.461 and –1.233	1.306 and –0.645

### X-ray crystallographic studies

Single crystals of **C3**, **C4-CH<sub>3</sub>OH**, and **C9-CH<sub>3</sub>OH** suitable for X-ray analysis were obtained by laying diethyl ether or isopropyl alcohol on the CH<sub>3</sub>OH solutions at rt. Single-crystal X-ray diffractions for **C3**, **C4-CH<sub>3</sub>OH**, and **C9-CH<sub>3</sub>OH** were collected on an R-Axis Rapid IP diffractometer (Rigaku, Tokyo, Japan) with graphite-monochromated Mo Kα radiation (λ = 0.71073 Å) at 173(2) K. Cell parameters were obtained by global refinement of the positions of all collected reflections. Intensities were corrected for Lorentz and polarization effects and empirical absorption. The structures were solved by direct methods and refined by full-matrix least-squares on F<sup>2</sup> using the SHELXL-97 package.<sup>[11]</sup> All nonhydrogen atoms were refined anisotropically. Crystal data collection and refinement details are summarized in Table 4.

Cambridge Crystallographic Data Center (CCDC) structures 1029800, 1029801, and 1029802 contain the supplementary crystallographic data for complexes **C3**, **C4-CH<sub>3</sub>OH**, and **C9-CH<sub>3</sub>OH** in this paper. These data can be obtained free of charge from the CCDC via [www.ccdc.cam.ac.uk/data\\_request/cif](http://www.ccdc.cam.ac.uk/data_request/cif).

### Acknowledgements

This work was supported by the National Natural Science Foundation of China (51273202, 21374123, and U1362204).

**Keywords:** 4-arylimino-1,2,3-trihydroacridines · catalysts · ethylene · nickel(II) complexes · oligomerization

- [1] a) L. K. Johnson, C. M. Killian, M. Brookhart, *J. Am. Chem. Soc.* **1995**, *117*, 6414–6415; b) C. M. Killian, L. K. Johnson, M. Brookhart, *Organometallics* **1997**, *16*, 2005–2007.
- [2] a) O. S. Trofymchuk, D. V. Gutsulyak, C. Quintero, M. Parvez, C. G. Daniiliuc, W. E. Piers, R. S. Rojas, *Organometallics* **2013**, *32*, 7323–7333; b) Z. Li, W.-H. Sun, Z. Ma, Y. Hu, C. Shao, *Chin. Chem. Lett.* **2001**, *12*, 691–692; c) X. Tang, W.-H. Sun, T. Gao, J. Hou, J. Chen, W. Chen, *J. Organomet. Chem.* **2005**, *690*, 1570–1580; d) J. M. Benito, E. de Jesús, F. J. de La Mata, J. C. Flores, R. Gómez, P. Gómez-Sal, *Organometallics* **2006**, *25*, 3876–3887; e) T. Irrgang, S. Keller, H. Maisel, W. Kretschmer, R. Kempe, *Eur. J. Inorg. Chem.* **2007**, 4221–4228; f) T. Schareina, G. Hillebrand, H. Fuhrmann, R. Kempe, *Eur. J. Inorg. Chem.* **2001**, 2421–2426; g) T.-J. J. Kinnunen, M. Haukka, T. T. Pakkanen, T. A. Pakkanen, *J. Organomet. Chem.* **2000**, *613*, 257–262; h) L. P. Spencer, R. Altwer, P. Wei, L. Gelmini, J. Gauld, D. W. Stephan, *Organometallics* **2003**, *22*, 3841–3854; i) J. D. Azoulay, Y. Schneider, G. B. Galland, G. C. Bazan, *Chem. Commun.* **2009**, 6177–6179; j) D. Zhang, E. T. Nades, M. Brookhart, O. Daugulis, *Organometallics* **2013**, *32*, 5136–5143; k) L. Li, M. Jeon, S. Y. Kim, *J. Mol. Catal. A: Chem.* **2009**, *303*, 110–116; l) R. Gao, L. Xiao, X. Hao, W.-H. Sun, F. Wang, *Dalton Trans.* **2008**, 5645–5651; m) P. Hao, S. Zhang, W.-H. Sun, Q. Shi, S. Adewuyi, X. Lu, P. Li, *Organometallics* **2007**, *26*, 2439–2446.
- [3] a) W. Zhang, W.-H. Sun, C. Redshaw, *Dalton Trans.* **2013**, *42*, 8988–8997; b) R. Gao, W.-H. Sun, C. Redshaw, *Catal. Sci. Technol.* **2013**, *3*, 1172–1179.

- [4] a) T. V. Laine, U. Piironen, K. Lappalainen, M. Klinga, E. Aitola, M. Leskela, *J. Organomet. Chem.* **2000**, *606*, 112–114; b) T. V. Laine, K. Lappalainen, J. Liiimatta, E. Aitola, B. Lofgren, M. Leskela, *Macromol. Rapid Commun.* **1999**, *20*, 487–491.
- [5] W.-H. Sun, S. Song, B. Li, C. Redshaw, X. Hao, Y.-S. Li, F. Song, *Dalton Trans.* **2012**, *41*, 11999–12010.
- [6] a) E. Yue, L. Zhang, Q. Xing, X.-P. Cao, X. Hao, C. Redshaw, W.-H. Sun, *Dalton Trans.* **2014**, *43*, 423–431; b) E. Yue, Q. Xing, L. Zhang, Q. Shi, X.-P. Cao, L. Wang, C. Redshaw, W.-H. Sun, *Dalton Trans.* **2014**, *43*, 3339–3346.
- [7] a) S. Song, T. Xiao, L. Wang, C. Redshaw, F. Wang, W.-H. Sun, *J. Organomet. Chem.* **2012**, *699*, 18–25; b) S. Song, Y. Li, C. Redshaw, F. Wang, W.-H. Sun, *J. Organomet. Chem.* **2011**, *696*, 3772–3778.
- [8] a) J. Yu, Y. Zeng, W. Huang, X. Hao, W.-H. Sun, *Dalton Trans.* **2011**, *40*, 8436–8443; b) X. Hou, Z. Cai, X. Chen, L. Wang, C. Redshaw, W.-H. Sun, *Dalton Trans.* **2012**, *41*, 1617–1623; c) L. Zhang, X. Hao, W.-H. Sun, C. Redshaw, *ACS Catal.* **2011**, *1*, 1213–1220.
- [9] S. A. Svejda, M. Brookhart, *Organometallics* **1999**, *18*, 65–74.
- [10] a) J. Lai, X. Hou, Y. Liu, C. Redshaw, W.-H. Sun, *J. Organomet. Chem.* **2012**, *702*, 52–58; b) F. He, X. Hao, X. Cao, C. Redshaw, W.-H. Sun, *J. Organomet. Chem.* **2012**, *712*, 46–51.
- [11] G. M. Sheldrick, SHELXL-97, Program for the Refinement of Crystal Structures, University of Göttingen, Göttingen (Germany), **1997**.

---

 Received: November 18, 2014

Published online on January 23, 2015